Articles

Diverse Regulation of SNF2h Chromatin Remodeling by Noncatalytic Subunits

Xi He,[‡] Hua-Ying Fan,[§] Joseph D. Garlick, and Robert E. Kingston*

Department of Molecular Biology, Massachusetts General Hospital, and Department of Genetics, Harvard Medical School, Boston, Massachusetts 02114

Received November 21, 2007; Revised Manuscript Received April 15, 2008

ABSTRACT: SNF2h-based ATP-dependent chromatin remodeling complexes diverge in composition, nuclear localization, and biological function. Such differences have led to the hypothesis that SNF2h complexes differ mechanistically. One proposal is that the complexes have different functional interactions with the naked DNA adjacent to the nucleosome. We have used a series of templates with defined nucleosomal position and differing amounts and placement of adjacent DNA to compare the relative activities of SNF2h and SNF2h complexes. The complexes hACF, CHRAC, WICH, and RSF all displayed differences in functional interactions with these templates, which we attribute to the differences in the noncatalytic subunit. We suggest that the ability to sense adjacent DNA is a general property of the binding partners of SNF2h and that each partner provides distinct regulation that contributes to distinct cellular function.

Modulation of chromatin structure is a key regulatory mechanism for many cellular processes. Chromatin can be modified via covalent (e.g., histone methylation, acetylation, etc.) or noncovalent pathways. One prevalent noncovalent modification uses the energy of ATP hydrolysis to alter nucleosome position and/or structure. ATP-dependent chromatin remodeling complexes are subdivided into several subfamilies based upon the identity of their ATPase subunit. The largest of these is the ISWI (imitation switch) subfamily, components of which are conserved from yeast to humans (*1, 2*).

The human ISWI isoforms are called SNF2h (sucrose nonfermenting 2 homologue) and SNF2L (sucrose nonfermenting 2-like), both of which are normally found in small protein complexes with auxiliary factors. The SNF2h-based complexes examined in this study are hACF (human ATP-utilizing chromatin assembly and remodeling factor, consisting of hACF1, short for ATP-utilizing chromatin assembly and remodeling factor 1, and SNF2h, short for sucrose nonfermenting 2 homologue) (*3*), RSF (remodeling and spacing factor, consisting of Rsf1, short for remodeling and spacing factor 1, and SNF2h) (*4, 5*), CHRAC (chromatin accessibility complex, consisting of hACF1, SNF2h, p15, and p17) (*3, 6*), WICH (Williams syndrome transcription factor-imitation switch, consisting of WSTF, short for Williams syndrome transcription factor, and SNF2h) (*7*). Other SNF2h complexes include NoRC [nucleolar remodeling complex, consisting of human TIP5 (transcription termination factor 1 interacting protein 5) and SNF2h] (*8*) and WCRF [Williams syndrome transcription factor-related chromatin remodeling factor, consisting of WCRF180 (Williams syndrome transcription factor-related chromatin remodeling factor 180) and SNF2h] (*9*). The only characterized SNF2L-based complex is NURF [nucleosome remodeling factor, consisting of BPTF (bromodomain PHD finger transcription factor), RbAP46/48 (retinoblastoma-associated protein 48 and 46), and SNF2L] (*10*). Several noncatalytic binding partners of SNF2h, including hACF1, WSTF, TIP5, and WCRF180, belong to the BAZ (bromodomain adjacent zinc finger) family (*11, 12*) (summarized in Table 1).

SNF2h has been shown to be essential for mouse development, as well as for individual cell survival (*13*). Furthermore, each of the different SNF2h complexes appears to have distinct biological functions (summarized in Table 2). The human ACF (hACF) complex has been shown to be involved in the replication of heterochromatin (*14*). This function may arise from the ability of hACF (as well as CHRAC and WICH complexes) to generate regularly spaced nucleosomal arrays in vitro (*4, 6, 7, 15–19*). While the WICH complex is involved in activating rDNA transcription (*20, 21*), the NoRC complex was shown to have a negative effect on the same process (*22, 23*). The RSF complex was shown to be amplified in gene copy as well as increased in transcription level in breast cancer cells (*24, 25*). The in vivo functions of CHRAC and WCRF remain less clearly defined; however, studies of the homologous complexes in *Drosophila* indicate that each human complex might also have specialized functions. For instance, the *Drosophila* NURF complex was shown to be able to activate transcription (*26*), while the dACF complex was shown to have a role in the global ability to space chromatin (*27, 28*). In addition, human RSF has been found to activate transcription in vitro (*5*).

* To whom correspondence should be addressed. Telephone: (617) 726-5990. Fax: (617) 726-5949. E-mail: Kingston@molbio.mgh.harvard.edu.

[‡] Current address: Department of Biochemistry, Tufts University, 136 Harrison Ave., Boston, MA 02111.

[§] Current address: Institute for Cancer Research, Fox Chase Cancer Center, 333 Cottman Ave., W470, Philadelphia, PA 19111.

10.1021/bi702304p CCC: $40.75
Published on Web 06/14/2008

Table 1: Human ISWI-Based Complexes

complex	subunit(s)
hACF (ATP-utilizing chromatin assembly and remodeling factor) (*2*)	SNF2h (sucrose nonfermenting 2 homologue) hACF1 (ATP-utilizing chromatin assembly and remodeling factor 1), belongs to the BAZ (bromodomain adjacent zinc finger) family (*11, 12*)
CHRAC (chromatin accessibility complex) (*3, 6*)	SNF2h, hACF1, p15, p17
WICH (WSTF-imitation switch) (*7*)	SNF2h WSTF (Williams syndrome transcription factor), belongs to the BAZ family (*11, 12*)
RSF (remodeling and spacing factor) (*4, 5*)	SNF2h Rsf1 (remodeling and spacing factor 1)
NoRC (nucleolar remodeling complex) (*8*)	SNF2h TIP5 (transcription termination factor 1 interacting protein 5), belongs to the BAZ family (*11, 12*)
WCRF (Williams syndrome transcription factor-related chromatin remodeling factor) (*9*)	SNF2h WCRF180 (Williams syndrome transcription factor-related chromatin remodeling factor 180), belongs to the BAZ family (*11, 12*)
NURF (nucleosome remodeling factor) (*10*)	SNF2L (sucrose nonfermenting 2-like) BPTF (bromodomain PHD finger transcription factor) RbAP46/48 (retinoblastoma-associated protein 48 and 46)

Table 2: Human ISWI-Based Complexes and Their Functions

complex	in vivo function	in vitro activity
hACF	heterochromatin replication (*14*)	spacing, transcription repression (*6*)
CHRAC	*a*	spacing (*6*)
WICH	rDNA transcription (*7, 21*)	spacing, transcription activation (*7, 20, 21*)
RSF	amplified gene copy and elevated transcription correlates with breast cancer (*24, 25*)	spacing (*4*), transcription activation (*5*)
NoRC	rDNA repression (*8, 23, 24*)	chromatin remodeling (*8*)
WCRF	*a*	*a*
NURF	transcription activation (*10*)	chromatin remodeling (*10*)

[a] Undefined.

We hypothesize that the functional differences between human SNF2h complexes may be caused, at least in part, by differential remodeling effects imparted by their noncatalytic subunits. Recent studies by us and others have shown that addition of the hACF1 subunit can alter the intrinsic remodeling activity of the SNF2h ATPase (*18, 19*). Specifically, hACF1 was shown to alter the length of flanking DNA (not associated with the histone octamer) required for productive remodeling (*18, 19, 29, 30*). These studies have led to proposals that hACF1 could play a mechanistic role in the nucleosome spacing effects of the hACF complex.

In this paper, we address the larger question of whether the different noncatalytic subunits of human SNF2h complexes cause distinct remodeling effects that might underlie the divergent functions of these complexes. Our results show characteristic differences in the ability of different SNF2h complexes to interact with and remodel nucleosomes containing varying amounts of flanking DNA. These results suggest that different subunits may alter SNF2h complex functions by regulating how each complex responds to flanking DNA.

EXPERIMENTAL PROCEDURES

Construction of DNA Templates. A *Pst*I site was engineered into different positions of the 601 template using the Stratagene QuikChange kit (*18*).

Protein Purification. The remodelers were expressed in Sf9 cells using pFASTBAC and purified by M2 affinity chromatography (*30, 31*): SNF2h (by expressing C-terminally FLAG-tagged SNF2h), hACF (by co-expressing C-terminal Flag-hACF1 and untagged SNF2h), CHRAC (C-terminal Flag-hACF1, untagged p15 and p17, and SNF2h), WICH (C-terminal Flag-WSTF and untagged SNF2h), and RSF (C-terminal Flag-Rsf1 and untagged SNF2h). The original hACF1 and WSTF cDNA clones were provided by P. Varga-Weisz. Clones of p15 and p17 were obtained from Invitrogen. The original Rsf1 cDNA clone was provided by D. Reinberg.

Mononucleosome Assembly and Purification. DNA templates were generated by PCR from the 601 sequence and body-labeled with [α-^{32}P]dATP. The nomenclatures of the nucleosomes are described in Figures 2A, 3A, and 4. The primers for the nucleosome that has no DNA overhang (C) are 5′-CCTGG AGAAT CCCGG TGCCG-3′ (forward) and 5′-CACAG GATGT ATATA TCTGA CACGT GCC-3′ (reverse). The primers for C20 (nucleosomes that have a 20 bp overhang) are 5′-CCTGG AGAAT CCCGG TGCCG-3′ (forward) and 5′-AAG GTC GCT GTT CAA TAC ATG C-3′ (reverse). The primers for C25 (nucleosomes with a 25 bp overhang and so on) are 5′-CCTGG AGAAT CCCGG TGCCG-3′ (forward) and 5′-CGGCA AGGTC GCTGT TC-3′ (reverse). The primers for C30 are 5′-CCTGG AGAAT CCCGG TGCCG-3′ (forward) and 5′-GGCAC CGGCA AGGTC GC-3′ (reverse). The primers for C35 are 5′-CCTGG AGAAT CCCGG TGCCG-3′ (forward) and 5′-CGACT GGCAC CGGCA AG-3′ (reverse). The primers for C40 are 5′-CCTGG AGAAT CCCGG TGCCG-3′ (forward) and 5′-TATCC GACTG GCACC GGC-3′ (reverse). The primers for C45 are 5′-CCTGG AGAAT CCCGG TGCCG-3′ (forward) and 5′-TCGGA ACACT ATCCG ACTGG CAC-3′ (reverse). The primers for C91 are 5′-CCTGG AGAAT CCCGG TGCCG-3′ (forward) and 5′-GGGCG AATTC GAGCT CGGTA CC-3′ (reverse). The primers for C120 are 5′-CCTGG AGAAT CCCGG TGCCG-3′ (forward) and 5′-CCAGT GAATT GTAAT ACGAC TCACT ATAG-3′ (reverse). The primers for 25C25 (nucleosomes that have 25 bp overhangs on both ends of the nucleosomal DNA) are 5′-TGTGA TGGAC CCTA TACGC G-3′ (forward) and 5′-CGGCA AGGTC GCTGT TC-3′ (reverse). The primers for 30C30 (nucleosomes that have 30 bp overhangs on both ends of the nucleosomal DNA and so forth) are 5′-CCCTT ATGTG ATGGA CCCTA TACGC-3′ (forward) and 5′-CTGGC ACCGG CAAGG TCGC-3′ (reverse). The primers for 45C45 are 5′-CACAC CGAGT TCATC CCTTA TGTGA-3′ (forward) and 5′-TCGGA ACACT ATCCG ACTGG CAC-3′ (reverse). The primers for 50C50 are 5′-TTCTT CACAC CGAGT TCATC CCTTA TGTG-3′ (forward) and 5′-GAGCT CGGAA CACTA TCCGA CTG-3′ (reverse). The primers for 55C55 are 5′-GGCAT GATTC TTCAC

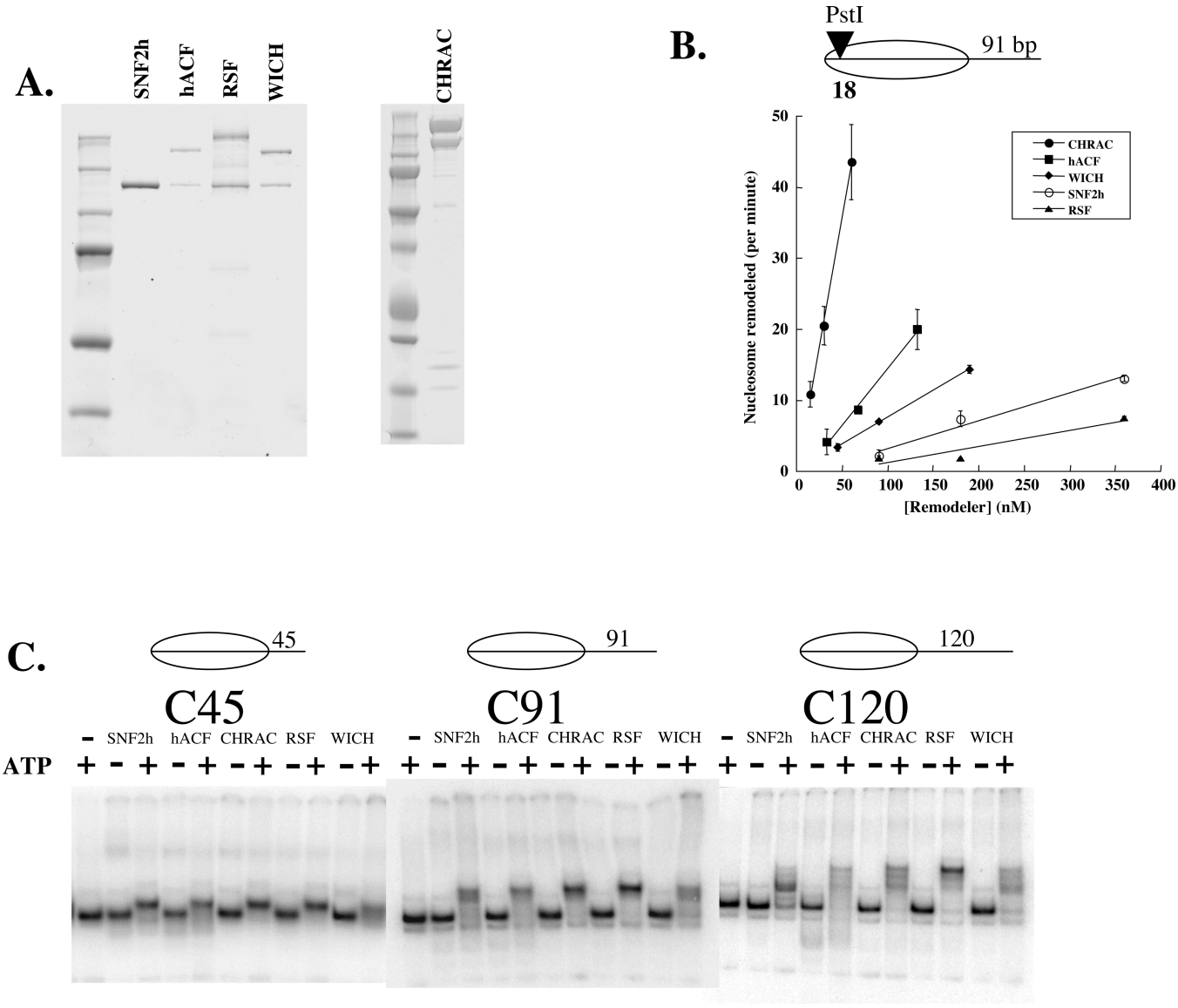

FIGURE 1: SNF2h and SNF2h-based complexes differ in their remodeling behaviors. (A) Coomassie stain of purified SNF2h, hACF, RSF, WICH, and CHRAC. (B) Measurement of the specific activity of SNF2h and SNF2h-based complexes. In the restriction enzyme accessibility assay, unlabeled C91 mononucleosomes were mixed with radiolabeled C91-18 (which had 91 bp of nucleosomal overhang from one end of the nucleosomal DNA and a unique *Pst*I site that was located 18 bp from the other end) to achieve the final concentration of 500 nM. Varying amounts of SNF2h (○), hACF (■), CHRAC (●), WICH (◆), and RSF (▲) were used in each reaction. (C) SNF2h and complexes generate different distributions of products on longer templates. In the nucleosome mobility shift assay, remodelers were used in excess (50 nM SNF2h, 15 nM hACF, 15 nM RSF, 15 nM WICH, and 7.5 nM CHRAC) over <1 nM labeled substrates with an overhang of 45 (C45), 91 (C91), or 120 bp (C120).

ACCGA GTTCATC-3′ (forward) and 5′-AGTGG GAGCT CGGAA CACTA TCC-3′ (reverse). The primers for 60C60 are 5′-GGAAA GCATG ATTCT TCACA CCGAG TTC-3′ (forward) and 5′-GCAGG TCGGG AGCTC GGAAC AC-3′ (reverse). The primers for 75C75 are 5′-GATCC TAATG ACCAA GGAAA GCATG ATTC-3′ (forward) and 5′-CAAGC TTGCA TGCCT GCAGG TC-3′ (reverse). The primers for 90C90 are 5′-GATCC TCTAG AGTCC GGGAT CC-3′ (forward) and 5′-GGGCG AATTC GAGCT CGGTA CC-3′ (reverse). The primers for 110C110 are 5′-TAGAA TACTC AAGCT TGCAT GCC-3′ (forward) and 5′-GTAAT ACGAC TCACT ATAGG GCGAA TTC-3′ (reverse). The primers for 30C90 are 5′-CCCTT ATGTG ATGGA CCCTA TACGC-3′ (forward) and 5′-GGGCG AATTC GAGCT CGGTA CC-3′ (reverse). The primers for 90C30 are 5′-GATCC TCTAG AGTCC GGGAT CC-3′ (forward) and 5′-CTGGC ACCGG CAAGG TCGC-3′ (reverse). The templates were assembled into mononucleosomes with HeLa core histones by step gradient salt dialysis, followed by purification on a 10 to 30% glycerol gradient (*18, 29–31*).

Nucleosome Mobility Assay. All reactions were performed as previously described (*29*); 50 nM SNF2h, 15 nM hACF, 15 nM CHRAC, 30 nM WICH, 50 nM RSF, and <1 nM labeled substrates were used in the reactions.

Restriction Enzyme Accessibility Assays (ATP-Dependent Remodeling Assay). All reaction mixtures contained remodelers in excess of nucleosomal substrates (<1 nM) to drive reactions to completion (except for specific activity determinations); 50 nM SNF2h, 15 nM hACF, 15 nM CHRAC, 30 nM WICH, 50 nM RSF, and <1 nM labeled substrates were used in the reactions. Other conditions were as previously described (*31*). The concentration of restriction enzyme *Pst*I used was determined to be non-rate-limiting (*31*). For the remodelers' specific activity determinations,

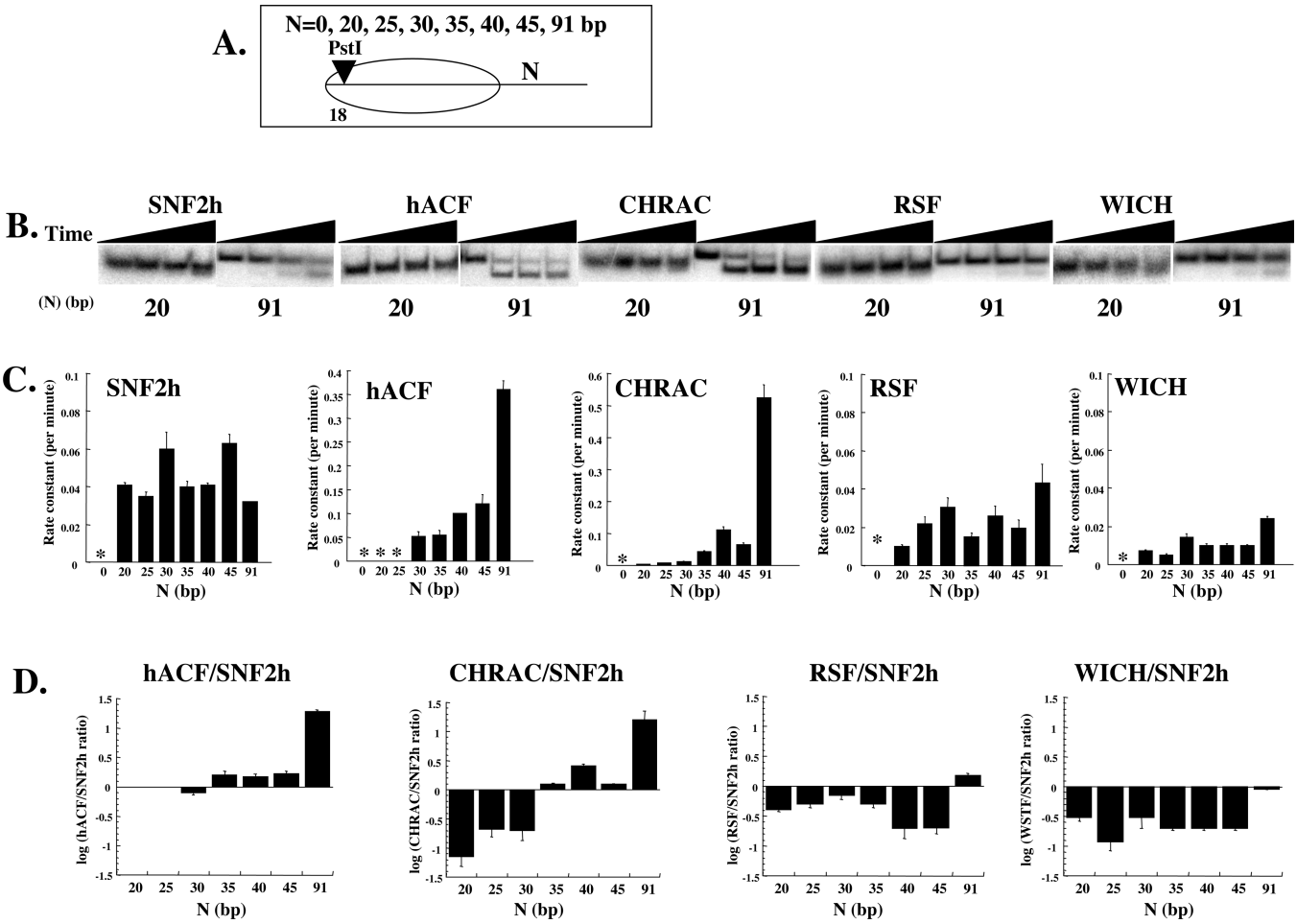

FIGURE 2: SNF2h complexes exhibit different remodeling profiles on end-positioned nucleosomes. (A) The end-positioned nucleosomes used here all have a unique *Pst*I site that is 18 bp from the end of the nucleosomal DNA. N denotes the overhang length (0, 20, 25, 30, 35, 40, 45, and 91 bp), CN the nucleosome, and 18 the position of the *Pst*I site (such as C-18, C20-18, C25-18, C30-18, C35-18, C40-18, C45-18, and C91-18). (B) SNF2h and complexes require different lengths of the nucleosomal DNA overhang. The restriction enzyme accessibility assay was used. Displayed here are the remodeling of C20-18 and C91-18 by SNF2h and complexes; 50 nM SNF2h, 15 nM hACF, 15 nM RSF, 15 nM WICH, and 7.5 nM CHRAC were used in excess of <1 nM nucleosomes in all reactions. (C) Different remodeling profiles of SNF2h and complexes. Remodelers (50 nM SNF2h, 15 nM hACF, 15 nM RSF, and 7.5 nM CHRAC) were used in excess over <1 nM substrates in the restriction enzyme accessibility assay. Asterisks mark the positions with no observed ATP-dependent increase in the remodeling rate constant. (D) Comparison of SNF2h-based remodeling on end-positioned nucleosomes. Ratios between the remodeling rate of SNF2h and a complex for each nucleosomal substrate were taken (complex/SNF2h). Log values were calculated for each ratio and then plotted against the length of the nucleosome DNA overhangs.

500 nM nucleosomes and varying amounts of remodelers were used in each reaction.

Electrophoretic Mobility Shift Assay. Reaction mixtures (10 μL) containing 10 fmol of radiolabeled nucleosomes (2.5 nM) were incubated with various amounts of remodeler in 80 mM KCl, 480 μM EDTA (pH 8.0), 20 mM Tris (pH 7.5), 14% glycerol, 4 mM $MgCl_2$, 0.4 μg/μL BSA, and 8 mM HEPES (pH 8.0). The reaction mixtures were incubated at 25 °C for 30 min before they were electrophoresed at 100 V for 3 h through 1.4% agarose gels in 0.4× TBE at room temperature. Gels were then dried and exposed to film (*32*).

RESULTS

The SNF2h protein and the remodeling complexes hACF, CHRAC, WICH, and RSF were expressed using baculoviruses and purified to homogeneity (Figure 1A). The activity of each complex was measured using a restriction enzyme accessibility assay. Previously occluded restriction enzyme sites in nucleosomal DNA are made accessible during a productive remodeling event. The rate of remodeling can be determined by measuring the rate of restriction enzyme cleavage under conditions of restriction enzyme excess (*31, 33, 34*). Here we used a mononucleosome with a 91 bp overhang at one end of the nucleosomal DNA and a *Pst*I site that was 18 bp from the other end. Each of the remodeling complexes and SNF2h were able to create access to the *Pst*I site in an ATP-dependent manner. The nucleosomal template was generated from the "601" nucleosome positioning sequence (see the next paragraph for details). Activity increased with an increasing concentration of remodeling complex (Figure 1B). CHRAC, hACF, and WICH exhibited higher levels of activity than SNF2h, demonstrating the activity of the added subunit. RSF and SNF2h exhibited similar levels of activity in this protocol (Figure 1B).

To further characterize the basic activity of these distinct complexes, we next used native gel electrophoresis to measure changes in the positioning of the remodeled nucleosome. Because a key aspect of this study involves different effects of overhanging DNA length on remodel-

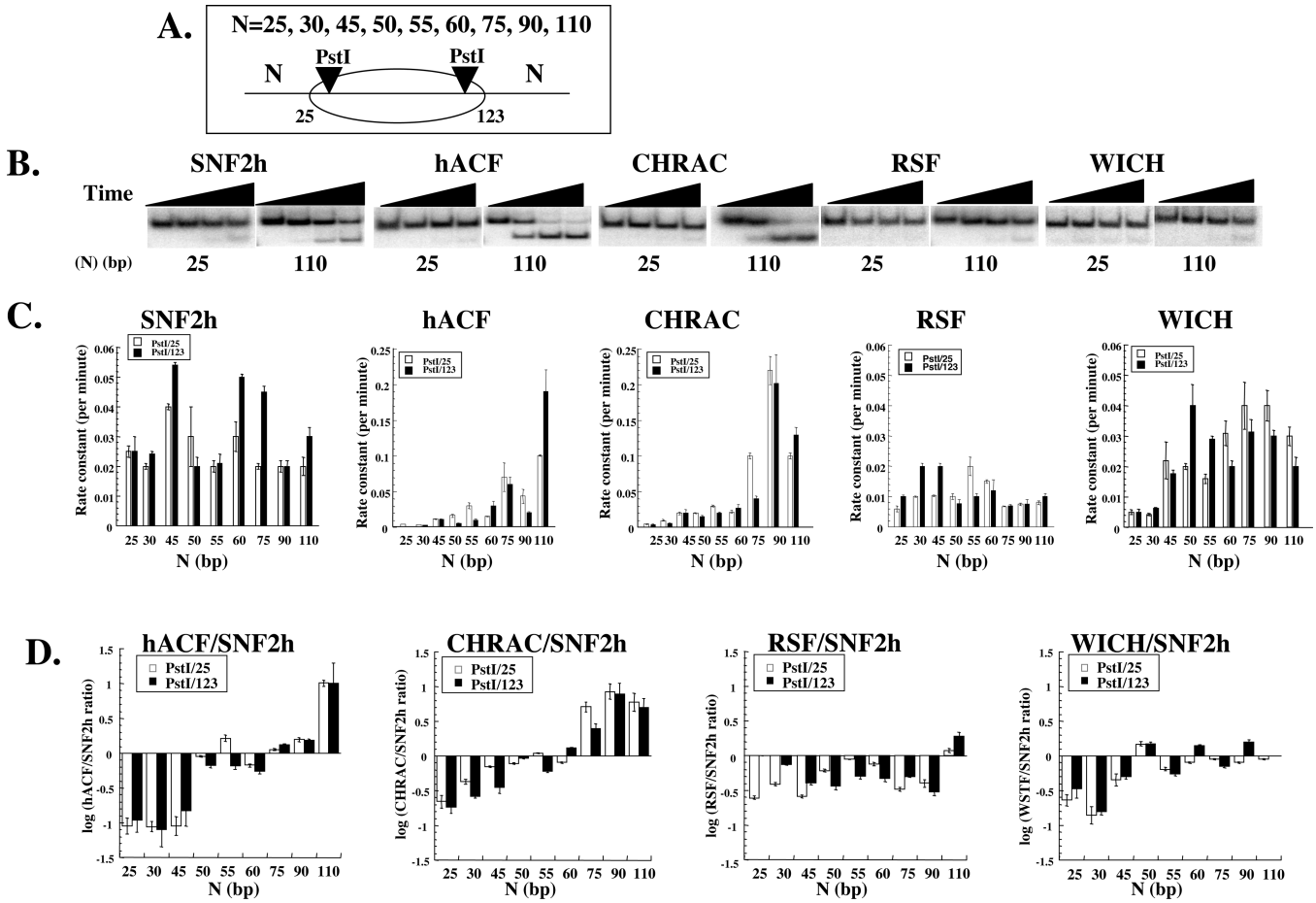

FIGURE 3: SNF2h complexes exhibit different remodeling patterns on symmetric nucleosomes. (A) Symmetric nucleosomes that were used in the profiling. Each template had a unique *Pst*I site at position 25 or 123 (25 or 123 bp, respectively, from the end of the nucleosomal DNA). *N* denotes the length of the DNA overhang (25, 30, 45, 50, 55, 60, 75, 90, and 110 bp); *NCN* denotes the templates (such as 25C25), and the number after the hyphen denotes the *Pst*I position (such as 25C25-25, 25C25-123, 30C30-25, 30C30-123, 45C45-25, 45C45-123, 50C50-25, 50C50-123, 55C55-25, 55C55-123, 60C60-25, 60C60-123, 75C75-25, 75C75-123, 90C90-25, 90C90-123, 110C110-25, and 110C110-123). (B) SNF2h and SNF2h complexes exhibit different remodeling profiles on 25C25-25 and 110C110-25 nucleosomes. The restriction enzyme accessibility assay was used; 50 nM SNF2h, 15 nM hACF, 15 nM RSF, 15 nM WICH, and 7.5 nM CHRAC were used in excess of <1 nM nucleosomes in all reactions. (C) SNF2h and SNF2h complexes have different profiles. Therefore, 50 nM SNF2h, 15 nM hACF, 15 nM RSF, 15 nM WICH, and 7.5 nM CHRAC were used in excess of <1 nM nucleosomes in all reactions. Asterisks mark the positions with no observed ATP-dependent increase in the remodeling rate constant. Remodeling rate constants at *Pst*I at position 25 are shown with white bars and those for *Pst*I at position 123 with black. (D) Comparison of remodeling on symmetric nucleosomes by SNF2h complexes. Ratios between the remodeling rate of SNF2h and a complex for each substrate were taken (complex/SNF2h). Log values were calculated for each ratio (*Pst*I at position 25, white; *Pst*I at position 123, black) and plotted against the length of the nucleosomal DNA overhangs.

ing (see below), we used the 601 nucleosome positioning sequence to generate templates (*18, 35*) that had a 45, 91, or 120 bp overhang at one end of the nucleosome (C45, C91, or C120, respectively) (Figure 1C). These templates were confirmed to contain uniformly positioned nucleosomes (*18*).

Each of the remodelers caused an ATP-dependent shift in mobility of each of the nucleosomes. Most of the SNF2h remodeled C45 nucleosome had a mobility that was consistent with a centrally localized nucleosome. On C91 and C120, SNF2h generated a greater diversity of products. In contrast, CHRAC and hACF remodeling generated mainly centrally localized nucleosomes on C45 and C91, but to a lesser extent on C120. WICH reactions exhibited a greater distribution of products than CHRAC and hACF. Interestingly, the RSF complex generated the most defined population of centrally localized nucleosomes on all templates (Figure 1C), which contrasts with its low specific activity as measured by the restriction enzyme accessibility assay (Figure 1B). These latter results also imply that the added subunit in the RSF complex is functioning to change the activity of SNF2h.

Differential Effects of Overhang DNA on Remodeling. It has been demonstrated that overhang DNA is essential for SNF2h-based remodeling (*18, 19, 29, 30*). SNF2h and hACF differ in the amount of DNA overhang that is optimal for their respective remodeling. This difference has been proposed to play a mechanistic role in nucleosome spacing. To assess the generality of this hypothesis, we determined the impact of overhang length on the rate of remodeling of the different SNF2h complexes. We used a series of defined substrates to measure their remodeling rates by using the restriction enzyme accessibility assay (*31, 33, 34*) (Figure 2A).

We constructed nucleosomal substrates that had an identical *Pst*I site that was 18 bp from the short end (the end without the DNA overhang) of the nucleosomal DNA (-18). The respective lengths of the DNA overhang were 0 (the overhang length was *N*; the substrate was C-18), 20 (C20-

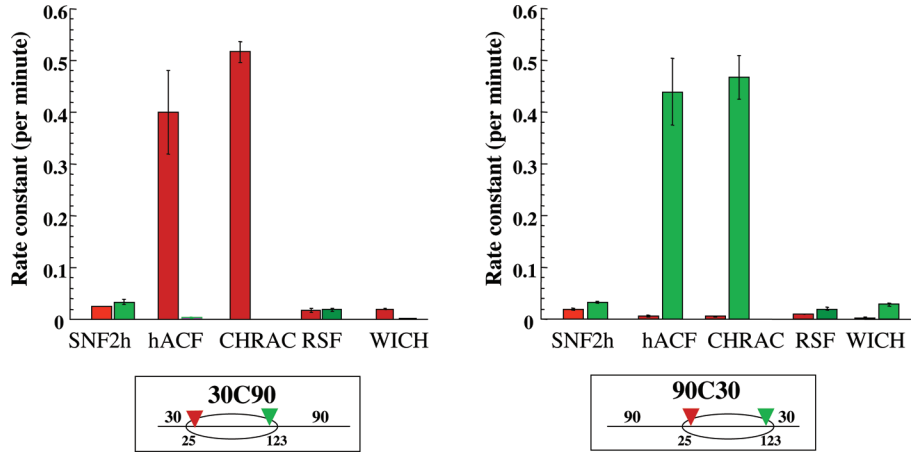

FIGURE 4: Different ability to center nucleosome by SNF2h complexes. Asymmetric substrates (30C90 and 90C30) were used to compare SNF2h-based remodeling in the restriction enzyme accessibility assay. Both sets of templates had a unique *Pst*I site at position 25 (red) or 123 (green), therefore consisting of 30C90-25 and 30C90-123, and 90C30-25 and 90C30-123 nucleosomes; 50 nM SNF2h, 15 nM hACF, 15 nM RSF, 15 nM WICH, and 7.5 nM CHRAC were used in excess of <1 nM nucleosomes in all reactions.

18), 25 (C25-18), 30 (C30-18), 35 (C35-18), 40 (C40-18), 45 (C45-18), and 91 bp (C91-18) (Figure 2A). We obtained remodeling rates for SNF2h and the complexes with each of the substrates by measuring the rate of creation of restriction enzyme access to each template under conditions of enzyme excess over substrate to drive each reaction to completion (Figure 2B). We and others have previously shown that these reaction conditions provide a reliable rate measurement for remodeling by this class of remodeling complexes (*29*). None of the remodelers could create access to the *Pst*I site in C-18 (Figure 2C and data not shown). This was consistent with the hypothesis that SNF2h-based remodeling requires the DNA overhang (*18, 30*). As observed previously, SNF2h could create access to the *Pst*I site on templates C20-18 and templates with overhangs longer than 20 (Figure 2B,C). The RSF and WICH complexes displayed behavior similar to that of SNF2h (Figure 2C). While hACF could create access on C30-18 and longer overhangs, the highly related CHRAC was active on C20-18 (Figure 2C). On C91-18, hACF and CHRAC had significantly greater rates than SNF2h, WICH, and RSF (Figure 2C).

To directly compare SNF2h remodeling to those of the complexes, a ratio was taken between the rate of each complex and SNF2h on each template (complex/SNF2h). This ratio was plotted against the length of the DNA overhang (*N*) (Figure 2D). hACF/SNF2h ratios started at C30-18, and CHRAC/SNF2h ratios started at C20-18. On shorter templates, SNF2h remodeling was significantly faster than that of hACF and CHRAC. Their remodeling rates became comparable on C40-18. On C91-18, hACF and CHRAC remodeling was significantly faster than that on SNF2h (Figure 2D). RSF remodeling differed from that of hACF and CHRAC, in that RSF/SNF2h ratios remained relatively constant (Figure 2D). Interestingly, on shorter templates, WICH/SNF2h ratios were similar to hACF/SNF2h and CHRAC/SNF2h ratios (Figure 2D). On C91-18, however, WICH/SNF2h and RSF/SNF2h ratios were similar (Figure 2D). We conclude that SNF2h and the SNF2h complexes varied in their requirement for nucleosomal overhang and that they exhibited diverse remodeling behaviors on templates of different lengths.

Remodeling on Templates with Symmetric DNA Overhangs. It has been proposed that the sensitivity of the SNF2h complex to nucleosomal overhang length is related to its ability to space nucleosomes (*18, 19*). To further compare the impact of overhang length on remodeling by each of the complexes, we constructed centrally positioned nucleosomes that contained different flanking overhangs [the overhang length was *N*; e.g., 25C25 (Figure 3A)]. In this manner, we were able to compare the impact of the total length of the overhang to the overhang position on SNF2h-based remodeling.

On each template, a unique *Pst*I site was engineered on the nucleosomal DNA at a position that was 25 or 123 bp from the end (e.g., 25C25-25 or 25C25-123, respectively) so that the *Pst*I sites were symmetrically positioned. We anticipated that the remodelers would create access to the 25 and 123 sites of the same template at comparable rates (*19*), and this prediction was confirmed (Figure 3C).

SNF2h and the complexes display similar remodeling patterns on the symmetric substrates as the end-positioned nucleosomes (Figures 2C and 3C). We verified that SNF2h remodeling did not display a dramatic change as nucleosomal overhang length changed (Figure 3C). Although hACF could not create access to *Pst*I site C25, it could open *Pst*I sites on 25C25 (Figure 3C). The total amount of DNA overhang, instead of the overhang length on one side, might be critical in affecting hACF remodeling (see Discussion). As in their profile with the end-positioned nucleosomes, hACF and CHRAC could remodel the 110C110 templates much faster than on shorter templates (Figure 3C).

The results were compared by plotting the log value of complex/SNF2h ratios against DNA overhang lengths (Figure 3D). Consistent with their ratio profiles on the end-positioned nucleosomes, both hACF and CHRAC remodeled shorter symmetric nucleosomes more slowly than SNF2h and faster than SNF2h on longer templates (Figure 3D). In addition, CHRAC remodeling demonstrated a more gradual increase in remodeling rates than hACF.

Interestingly, the remodeling rates of RSF did not appear to be affected by the DNA overhang lengths (Figure 3C), as the RSF/SNF2h ratios remained relatively constant (Figure 3D). On the other hand, WICH remodeling was similar to hACF and CHRAC remodeling on shorter templates but became more like RSF remodeling on longer templates (Figure 3D).

Remodeling on Templates with Asymmetric DNA Overhangs. A preference for remodeling on longer templates may correlate with chromatin spacing if the increase in the rate of remodeling causes the nucleosome to move preferentially onto the longer DNA overhang. To address this issue, we designed two templates: one with a 30 bp overhang on one side of the nucleosome and 90 bp on the other side (30C90) and the other with the positions of the overhangs reversed (90C30). Within each set of templates, there was a unique *Pst*I site at either position 25 or 123 in the nucleosomal DNA [e.g., 30C90-25 or 30C90-123, respectively (Figure 4)]. There was no significant difference between the rates of remodeling by SNF2h of these *Pst*I sites (Figure 4), which is consistent with the lack of impact of overhang length on SNF2h function. As observed previously, hACF had a dramatic preference for remodeling sites distal to the long overhang (Figure 4). CHRAC showed behavior similar to that of hACF. WICH also preferentially created access to sites distal to the long end, but to a lesser degree than hACF and CHRAC. hACF, CHRAC, and WICH appeared to preferentially move the nucleosome onto the longer DNA overhang and away from the shorter DNA overhang. Remodeling by RSF did not display such a preference (Figure 4). We conclude that the level of preference of these complexes to remodel sites distal to the long overhang correlates with the extent to which their activity is influenced by the length of the DNA overhang.

Different Interactions between SNF2h Complexes and Nucleosomes. From the results given above, we see that the SNF2h complexes differ in their requirement of an extranucleosomal DNA overhang for successful remodeling. In addition, we have previously demonstrated that the presence of hACF1 alters the interaction between SNF2h and nucleosomes by increasing the apparent affinity (*18*). To determine whether the other subunits examined here also increased the affinity for nucleosomal substrates, we used an electrophoretic mobility shift assay. We compared binding of the remodeling complexes to a nucleosome with no overhang (C) to one with a 120 bp overhang (C120). In the absence of a DNA overhang, SNF2h had weak interaction with the core nucleosome (Figure 5A), which remained weak (but perhaps slightly enhanced) in the presence of the 120 bp overhang [Figure 5B; the band(s) of nucleosome that has been shifted by its interaction with SNF2h is marked with an asterisk]. These interactions were significantly strengthened in the presence of a noncatalytic subunit. Each of the SNF2h-based complexes had stronger interactions with both the core and C120 nucleosomes [Figure 5A,B; the band(s) of nucleosome that has been shifted by its interaction with SNF2h complexes is marked with an asterisk]. The addition of an overhang did not increase the apparent affinity of binding of the complexes, indicating that the interaction of the complexes with the core nucleosome predominates under these conditions. These findings are consistent with the previous observation that the noncatalytic subunit enhanced the interaction between SNF2h and the nucleosomal substrate. While the presence of either a DNA overhang or a noncatalytic subunit has previously been shown to enhance the interaction between the ISWI ATPase and the nucleosome, it is possible that the noncatalytic subunit plays a predominant role (*6, 17, 18, 36*). As seen before, this increased affinity alone does not fully explain the impact of the overhang on remodeling, as it is seen even with nucleosomes that have no overhang and hence cannot be remodeled.

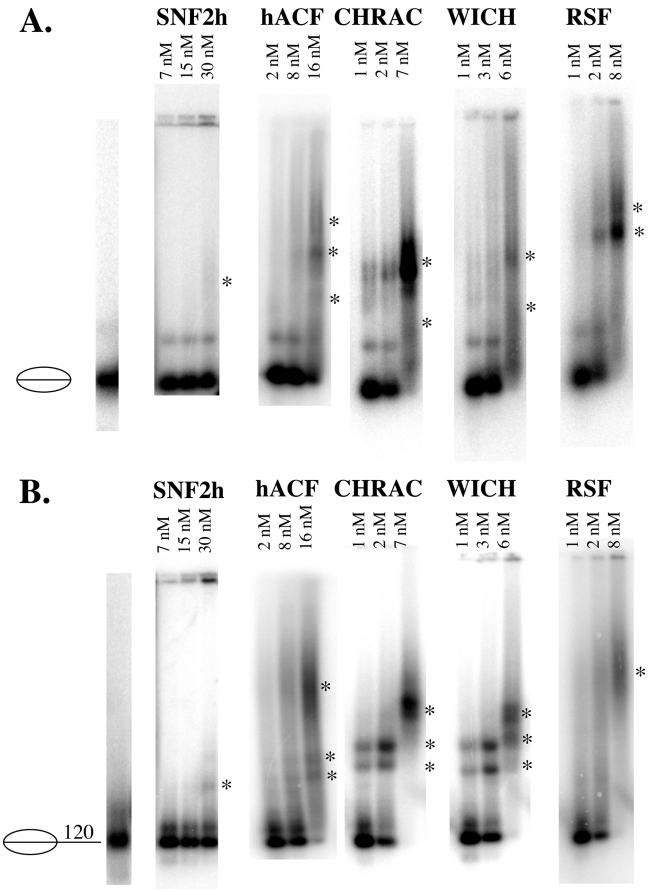

FIGURE 5: SNF2h complexes display different binding affinities for nucleosomes. Core nucleosomes (C) were assembled on radiolabeled 601 templates that consist of 149 bp, while C120 nucleosomes were assembled on radiolabeled 601 templates that consist of 269 bp. Nucleosomes (2.5 nM, 10 fmol per reaction) were incubated with increasing amounts of remodelers in the absence of ATP. Nucleosomes and nucleosome−remodeler complexes were separated by native agarose gel electrophoresis and visualized by autoradiography. Positions of the unbound nucleosomes are denoted with diagrams of C and C120, while nucleosome−remodeler complexes are denoted with asterisks.

DISCUSSION

It has been shown that the noncatalytic subunit of the hACF complex alters the functional requirement for adjacent naked DNA. Here we show that this observation extends to subunits in the CHRAC and WICH complexes, although there are characteristic differences among hACF, CHRAC, and WICH. In contrast, the RSF complex does not preferentially remodel templates with longer DNA overhangs. These data support the hypothesis that additional subunits alter the physical interaction between SNF2h and the DNA adjacent to the nucleosome. We propose that these characteristics are related to the ability to space nucleosomes in natural chromatin, where linker DNA is expected to play a mechanistic role similar to that of the nucleosomal overhang.

hACF exhibited very low remodeling activity on 25C25 through 45C45 templates, moderate activity on 50C50 through 90C90 templates, and ~3-fold enhanced activity on the 110C110 template (Figure 5). This is consistent with the

following model (a variant of one proposed in ref *19*). hACF has three classes of remodeling activities, depending on the length of flanking DNA. (1) With flanking DNA of ≤45 bp, low hACF remodeling activity prevents nucleosomes from being spaced too close to each other. (2) With flanking sequences between ~50 and ~90 bp, hACF remodels at a faster rate to achieve nucleosome spacing. (3) With even longer flanking DNA, hACF has a further increased rate of remodeling to allow for rapid nucleosome spacing. These observations could result from the hACF1 subunit interacting with SNF2h to alter its ability to remodel, from the hACF1 subunit interacting with the template to alter the efficiency with which nucleosomes can be moved along the template, or from a combination of both mechanisms. We favor the latter possibility, although the available data do not discriminate between these models. Similar arguments can be made concerning the role of the non-SNF2h subunits in the other complexes tested here.

In contrast to hACF, CHRAC appears to work in a more graded fashion, with activity gradually increasing up to the 90C90 template. In addition, CHRAC also appears to reach maximal activity earlier (at 90C90 instead of 110C110 for hACF). The difference in hACF and CHRAC remodeling can be attributed to the p15−p17 dimer, which is known to enhance the interaction between hACF and the nucleosome (*6*). The yeast homologues of p15 and p17, Dpb4 and Dls1, respectively, tether the Isw2 complex to extranucleosomal DNA, suggesting that these types of interactions also occur in yeast (*36*). The p15−p17 dimer might interact with the nucleosomal DNA to reduce the requirement for CHRAC remodeling by 10 bp. hACF and CHRAC remodeling might thereby generate different lengths of internucleosomal DNA in vivo.

WICH and RSF both exhibit very different flanking DNA effects when compared to those of hACF and CHRAC. This is true despite the fact that the major noncatalytic subunits of these complexes, WSTF, hACF1, and Rsf1, are homologues with similar domain structures [members of the BAZ family (*11, 12*)]. Our results indicate that, irrespective of these similarities, each of these subunits can confer distinct template preferences for remodeling. Thus, the regulatory relationships between SNF2h and its binding partners are too complex to be simply explained by distinct domains. This is consistent with observations that the regulation of *Drosophila* ISWI could not be fully explained by distinct domains in dAcf1 (*17, 37*). It is possible that the slight differences in the motifs, such as in the bromodomains and PHD domains in BAZ proteins, might contribute to their differential regulation of SNF2h (*38–41*).

The role of the nucleosomal DNA overhang in facilitating ISWI-based remodeling appears to be a shared characteristic in yeast, *Drosophila*, and humans (*18, 42, 43*). Furthermore, the alteration of the interaction between SNF2h and nucleosomes by noncatalytic subunits has been observed in different species (*17, 18, 36*). Finally, the role of the histone tail in SNF2h-based remodeling distinguishes the subfamily of SNF2h complexes from other subfamilies (*34, 44–47*). The general role for the DNA overhang in remodeling and the observation reported here that this effect changes with different complexes highlight the importance of the flanking DNA for the function of the ISWI family. While the experiments conducted here were purposefully done with artificial sequences (*35*), it is intriguing that biologically important sequences can also impact remodeling and even direct the nucleosome to a specific location following remodeling (*48, 49*). It will be interesting to determine whether different complexes also exhibit different sequence preferences in addition to the different length preferences that are reported here.

The findings reported here support the hypothesis that the different noncatalytic subunits regulate SNF2h activity differently, therefore generating different remodeling outcomes appropriate for the diverse in vivo roles of the SNF2h complexes. Transcriptionally active chromatin has been observed to have shorter internucleosomal DNA than repressed regions (*50–52*). Thus, the greater length required for hACF stimulation might contribute to a specialized function in providing the long repeat length of heterochromatin. Furthermore, WICH remodeling might generate chromatin with shorter spacer DNA, consistent with its role in transcriptional activation of the rDNA loci. Lastly, RSF might be more involved in transcriptional initiation events than the general spacing activity, accounting for the lack of preference for additional DNA. Taken together, these studies indicate that the noncatalytic subunits of hACF, CHRAC, WICH, and RSF alter the remodeling activity of SNF2h to generate different remodeling outcomes which are likely to be relevant to the divergent in vivo functions of these complexes.

ACKNOWLEDGMENT

We thank J. Widom for the 601 sequence, P. Varga-Weisz for the WSTF and hACF1 cDNA, and D. Reinberg for the Rsf1 cDNA and virus. X.H. thanks K. Bouazoune for technical assistance. We also thank K. Bouazoune, G. Schnitzler, C. Pham, and J. Sun for comments on the manuscript.

REFERENCES

1. Havas, K., Whitehouse, I., and Owen-Hughes, T. (2001) ATP-dependent chromatin remodeling activities. *Cell. Mol. Life Sci. 58*, 673–682.
2. Narlikar, G. J., Fan, H. Y., and Kingston, R. E. (2002) Cooperation between complexes that regulate chromatin structure and transcription. *Cell 108*, 475–487.
3. Poot, R. A., Dellaire, G., Hulsmann, B. B., Grimaldi, M. A., Corona, D. F., Becker, P. B., Bickmore, W. A., and Varga-Weisz, P. D. (2000) HuCHRAC, a human ISWI chromatin remodelling complex contains hACF1 and two novel histone-fold proteins. *EMBO J. 19*, 3377–3387.
4. Loyola, A., Huang, J. Y., LeRoy, G., Hu, S., Wang, Y. H., Donnelly, R. J., Lane, W. S., Lee, S. C., and Reinberg, D. (2003) Functional analysis of the subunits of the chromatin assembly factor RSF. *Mol. Cell. Biol. 23*, 6759–6768.
5. LeRoy, G., Orphanides, G., Lane, W. S., and Reinberg, D. (1998) Requirement of RSF and FACT for transcription of chromatin templates in vitro. *Science 282*, 1900–1904.
6. Kukimoto, I., Elderkin, S., Grimaldi, M., Oelgeschlager, T., and Varga-Weisz, P. D. (2004) The histone-fold protein complex CHRAC-15/17 enhances nucleosome sliding and assembly mediated by ACF. *Mol. Cell 13*, 265–277.
7. Bozhenok, L., Wade, P. A., and Varga-Weisz, P. (2002) WSTF-ISWI chromatin remodeling complex targets heterochromatic replication foci. *EMBO J. 21*, 2231–2241.
8. Strohner, R., Nemeth, A., Jansa, P., Hofmann-Rohrer, U., Santoro, R., Langst, G., and Grummt, I. (2001) NoRC: A novel member of mammalian ISWI-containing chromatin remodeling machines. *EMBO J. 20*, 4892–4900.
9. Bochar, D. A., Savard, J., Wang, W., Lafleur, D. W., Moore, P., Cote, J., and Shiekhattar, R. (2000) A family of chromatin

remodeling factors related to Williams syndrome transcription factor. *Proc. Natl. Acad. Sci. U.S.A. 97*, 1038–1043.
10. Barak, O., Lazzaro, M. A., Lane, W. S., Speicher, D. W., Picketts, D. J., and Shiekhattar, R. (2003) Isolation of human NURF: A regulator of Engrailed gene expression. *EMBO J. 22*, 6089–6100.
11. Jones, M. H., Hamana, N., Nezu, J., and Shimane, M. (2000) A novel family of bromodomain genes. *Genomics 63*, 40–45.
12. Doerks, T., Copley, R., and Bork, P. (2001) DDT: A novel domain in different transcription and chromosome remodeling factors. *Trends Biochem. Sci. 26*, 145–146.
13. Stopka, T., and Skoultchi, A. I. (2003) The ISWI ATPase Snf2h is required for early mouse development. *Proc. Natl. Acad. Sci. U.S.A. 100*, 14097–14102.
14. Collins, N., Poot, R. A., Kukimoto, I., Garcia-Jimenez, C., Dellaire, G., and Varga-Weisz, P. D. (2002) An ACF1-ISWI chromatin-remodeling complex is required for DNA replication through heterochromatin. *Nat. Genet. 32*, 627–632.
15. Vary, J. C., Jr., Fazzio, T. G., and Tsukiyama, T. (2004) Assembly of yeast chromatin using ISWI complexes. *Methods Enzymol. 375*, 88–102.
16. Ito, T., Levenstein, M. E., Fyodorov, D. V., Kutach, A. K., Kobayashi, R., and Kadonaga, J. T. (1999) ACF consists of two subunits, Acf1 and ISWI, that function cooperatively in the ATP-dependent catalysis of chromatin assembly. *Genes Dev. 13*, 1529–1539.
17. Fyodorov, D. V., and Kadonaga, J. T. (2002) Binding of Acf1 to DNA involves a WAC motif and is important for ACF-mediated chromatin assembly. *Mol. Cell. Biol. 22*, 6344–6353.
18. He, X., Fan, H. Y., Narlikar, G. J., and Kingston, R. E. (2006) Human ACF1 alters the remodeling strategy of SNF2h. *J. Biol. Chem. 281*, 28636–28647.
19. Yang, J. G., Madrid, T. S., Sevastopoulos, E., and Narlikar, G. J. (2006) The chromatin-remodeling enzyme ACF is an ATP-dependent DNA length sensor that regulates nucleosome spacing. *Nat. Struct. Mol. Biol. 13*, 1078–1083.
20. Cavellan, E., Asp, P., Percipalle, P., and Farrants, A. K. (2006) The WSTF-SNF2h chromatin remodeling complex interacts with several nuclear proteins in transcription. *J. Biol. Chem. 281*, 16264–16271.
21. Percipalle, P., Fomproix, N., Cavellan, E., Voit, R., Reimer, G., Kruger, T., Thyberg, J., Scheer, U., Grummt, I., and Farrants, A. K. (2006) The chromatin remodelling complex WSTF-SNF2h interacts with nuclear myosin 1 and has a role in RNA polymerase I transcription. *EMBO Rep. 7*, 525–530.
22. Santoro, R., and Grummt, I. (2005) Epigenetic mechanism of rRNA gene silencing: Temporal order of NoRC-mediated histone modification, chromatin remodeling, and DNA methylation. *Mol. Cell. Biol. 25*, 2539–2546.
23. Strohner, R., Nemeth, A., Nightingale, K. P., Grummt, I., Becker, P. B., and Langst, G. (2004) Recruitment of the nucleolar remodeling complex NoRC establishes ribosomal DNA silencing in chromatin. *Mol. Cell. Biol. 24*, 1791–1798.
24. Mao, T. L., Hsu, C. Y., Yen, M. J., Gilks, B., Sheu, J. J., Gabrielson, E., Vang, R., Cope, L., Kurman, R. J., Wang, T. L., and Shih Ie, M. (2006) Expression of Rsf-1, a chromatin-remodeling gene, in ovarian and breast carcinoma. *Hum. Pathol. 37*, 1169–1175.
25. Shih Ie, M., Sheu, J. J., Santillan, A., Nakayama, K., Yen, M. J., Bristow, R. E., Vang, R., Parmigiani, G., Kurman, R. J., Trope, C. G., Davidson, B., and Wang, T. L. (2005) Amplification of a chromatin remodeling gene, Rsf-1/HBXAP, in ovarian carcinoma. *Proc. Natl. Acad. Sci. U.S.A. 102*, 14004–14009.
26. Mizuguchi, G., Tsukiyama, T., Wisniewski, J., and Wu, C. (1997) Role of nucleosome remodeling factor NURF in transcriptional activation of chromatin. *Mol. Cell 1*, 141–150.
27. Fyodorov, D. V., Blower, M. D., Karpen, G. H., and Kadonaga, J. T. (2004) Acf1 confers unique activities to ACF/CHRAC and promotes the formation rather than disruption of chromatin in vivo. *Genes Dev. 18*, 170–183.
28. Ito, T., Bulger, M., Pazin, M. J., Kobayashi, R., and Kadonaga, J. T. (1997) ACF, an ISWI-containing and ATP-utilizing chromatin assembly and remodeling factor. *Cell 90*, 145–155.
29. Fan, H. Y., He, X., Kingston, R. E., and Narlikar, G. J. (2003) Distinct strategies to make nucleosomal DNA accessible. *Mol. Cell 11*, 1311–1322.
30. Aalfs, J. D., Narlikar, G. J., and Kingston, R. E. (2001) Functional differences between the human ATP-dependent nucleosome remodeling proteins BRG1 and SNF2H. *J. Biol. Chem. 276*, 34270–34278.
31. Narlikar, G. J., Phelan, M. L., and Kingston, R. E. (2001) Generation and interconversion of multiple distinct nucleosomal states as a mechanism for catalyzing chromatin fluidity. *Mol. Cell 8*, 1219–1230.
32. Bouazoune, K., and Brehm, A. (2005) dMi-2 chromatin binding and remodeling activities are regulated by dCK2 phosphorylation. *J. Biol. Chem. 280*, 41912–41920.
33. Polach, K. J., and Widom, J. (1999) Restriction enzymes as probes of nucleosome stability and dynamics. *Methods Enzymol. 304*, 278–298.
34. Logie, C., and Peterson, C. L. (1997) Catalytic activity of the yeast SWI/SNF complex on reconstituted nucleosome arrays. *EMBO J. 16*, 6772–6782.
35. Lowary, P. T., and Widom, J. (1998) New DNA sequence rules for high affinity binding to histone octamer and sequence-directed nucleosome positioning. *J. Mol. Biol. 276*, 19–42.
36. Dang, W., Kagalwala, M. N., and Bartholomew, B. (2007) The Dpb4 subunit of ISW2 is anchored to extranucleosomal DNA. *J. Biol. Chem. 282*, 19418–19425.
37. Eberharter, A., Vetter, I., Ferreira, R., and Becker, P. B. (2004) ACF1 improves the effectiveness of nucleosome mobilization by ISWI through PHD-histone contacts. *EMBO J. 23*, 4029–4039.
38. Fujiki, R., Kim, M. S., Sasaki, Y., Yoshimura, K., Kitagawa, H., and Kato, S. (2005) Ligand-induced transrepression by VDR through association of WSTF with acetylated histones. *EMBO J. 24*, 3881–3894.
39. Hassan, A. H., Prochasson, P., Neely, K. E., Galasinski, S. C., Chandy, M., Carrozza, M. J., and Workman, J. L. (2002) Function and selectivity of bromodomains in anchoring chromatin-modifying complexes to promoter nucleosomes. *Cell 111*, 369–379.
40. Matangkasombut, O., and Buratowski, S. (2003) Different sensitivities of bromodomain factors 1 and 2 to histone H4 acetylation. *Mol. Cell 11*, 353–363.
41. Zhou, Y., and Grummt, I. (2005) The PHD finger/bromodomain of NoRC interacts with acetylated histone H4K16 and is sufficient for rDNA silencing. *Curr. Biol. 15*, 1434–1438.
42. Kagalwala, M. N., Glaus, B. J., Dang, W., Zofall, M., and Bartholomew, B. (2004) Topography of the ISW2-nucleosome complex: Insights into nucleosome spacing and chromatin remodeling. *EMBO J. 23*, 2092–2104.
43. Whitehouse, I., Stockdale, C., Flaus, A., Szczelkun, M. D., and Owen-Hughes, T. (2003) Evidence for DNA translocation by the ISWI chromatin-remodeling enzyme. *Mol. Cell. Biol. 23*, 1935–1945.
44. Clapier, C. R., Langst, G., Corona, D. F., Becker, P. B., and Nightingale, K. P. (2001) Critical role for the histone H4 N terminus in nucleosome remodeling by ISWI. *Mol. Cell. Biol. 21*, 875–883.
45. Clapier, C. R., Nightingale, K. P., and Becker, P. B. (2002) A critical epitope for substrate recognition by the nucleosome remodeling ATPase ISWI. *Nucleic Acids Res. 30*, 649–655.
46. Guyon, J. R., Narlikar, G. J., Sif, S., and Kingston, R. E. (1999) Stable remodeling of tailless nucleosomes by the human SWI-SNF complex. *Mol. Cell. Biol. 19*, 2088–2097.
47. Logie, C., Tse, C., Hansen, J. C., and Peterson, C. L. (1999) The core histone N-terminal domains are required for multiple rounds of catalytic chromatin remodeling by the SWI/SNF and RSC complexes. *Biochemistry 38*, 2514–2522.
48. Rippe, K., Schrader, A., Riede, P., Strohner, R., Lehmann, E., and Langst, G. (2007) DNA sequence- and conformation-directed positioning of nucleosomes by chromatin-remodeling complexes. *Proc. Natl. Acad. Sci. U.S.A. 104*, 15635–15640.
49. Sims, H. I., Lane, J. M., Ulyanova, N. P., and Schnitzler, G. R. (2007) Human SWI/SNF drives sequence-directed repositioning of nucleosomes on C-myc promoter DNA minicircles. *Biochemistry 46*, 11377–11388.
50. Villeponteau, B., Brawley, J., and Martinson, H. G. (1992) Nucleosome spacing is compressed in active chromatin domains of chick erythroid cells. *Biochemistry 31*, 1554–1563.
51. Gottschling, D. E., Palen, T. E., and Cech, T. R. (1983) Different nucleosome spacing in transcribed and non-transcribed regions of the ribosomal RNA gene in *Tetrahymena thermophila*. *Nucleic Acids Res. 11*, 2093–2109.
52. Berkowitz, E. M., and Riggs, E. A. (1981) Characterization of rat liver oligonucleosomes enriched in transcriptionally active genes: Evidence for altered base composition and a shortened nucleosome repeat. *Biochemistry 20*, 7284–7290.

BI702304P